Immunolocalization of zinc transporters and metallothioneins reveals links to microvascular morphology and functions

Hai Bac Tran (haibac.tran@adelaide.edu.au)
University of Adelaide
Rachel Jakobczak
University of Adelaide
Adrian Abdo
University of Adelaide
Patrick Asare
University of Adelaide
Paul Reynolds
University of Adelaide
John Beltrame
University of Adelaide
Sandra Hodge
University of Adelaide
Peter Zalewski
University of Adelaide

Research Article

Keywords: Vascular dysfunction, pulmonary arterial hypertension, SLC39A/ZIPs zinc transporters, ZIP12, metallothioneins, multifluorescence quantitative confocal microscopy

Posted Date: April 13th, 2022

DOI: https://doi.org/10.21203/rs.3.rs-1539166/v1

Abstract

Zinc homeostasis is vital to immune and other organ system functions, yet over a quarter of the world's population are zinc deficient. Abnormal zinc transport or storage protein expression has been linked to diseases, such as cancer and chronic obstructive pulmonary disorder. Although recent studies indicate a role for zinc regulation in vascular functions and diseases, detailed knowledge of the mechanisms involved remain unknown. This study aimed to assess protein expression and localization of zinc transporters of the SLC39A/ZIP family (ZIPs) and metallothioneins (MTs) in human subcutaneous microvessels, and to relate them to morphologic features and expression of function-related molecules in the microvasculature. Microvessels in paraffin biopsies of subcutaneous adipose tissues from 14 patients undergoing hernia reconstruction surgery were analysed for 9 ZIPs and 3 MT proteins by MQCM (multifluorescence quantitative confocal microscopy). Zinc regulation proteins detected in human microvasculature included ZIP1, ZIP2, ZIP8, ZIP10, ZIP12, ZIP14, and MT1-3, which showed differential localization among endothelial and smooth muscle cells. ZIP1, ZIP2, ZIP12 and MT3 showed significantly ($p < 0.05$) increased immunoreactivities, in association with increased microvascular muscularization, and upregulated ET-1, α-SMA and the active form of p38 MAPK (Thr180/Tyr182 phosphorylated, p38 MAPK-P). These findings support roles of the zinc regulation system in microvascular physiology and diseases.

Introduction

The complex system of small blood vessels, namely arterioles, capillaries and venules, collectively called microvessels, is central in life-threatening conditions such as pulmonary arterial hypertension (PAH), coronary microvascular disease and microvascular brain disease. The microvascular wall consists of a few cell types, of which endothelial cells and smooth muscle cells are the two major populations in arterioles (diameter 10–100 μm), and venules (12–400 μm). In adult healthy microvessels, both these cell types are relatively quiescent, not proliferating, but sensitive to chemical or mechanical stimuli for activation (Ricard et al. 2021; Ourne et al. 2021). This activation may lead to increased cell proliferation and even switching the smooth muscle cell phenotype (Ourne et al. 2021; Bkaily et al. 2021), resulting in a broad range of morphological and physiological changes known as "vascular remodelling" (Mulvany 1999). In animal models of diabetes and metabolic syndrome, hypertrophic remodelling of microvessels was identified in early stages, when coronary arteries remained normal by angiography, indicating a key role for remodelling of micro- rather than macrovessels in initiation of hemodynamic disorders in these disease (Lambazi & Trask 2017). Multiple cellular and molecular events are ascribed to mechanisms of microvascular remodelling in pulmonary arterial hypertension, including proliferation and hypertrophy of smooth muscle cells, instigated in particular by signalling cascades with calcium (Mandegar et al. 2004), hypoxia-induced factor (Liu et al. 2019), sphingosine-1-phosphate (Ranasinghe et al. 2020) etc.

Zinc homeostasis is vital for functioning of the immune and other organs and systems. Cellular zinc homeostasis is regulated by three major families of proteins: (i) Solute Carrier 39 family/Zrt- and Irt-like proteins (SLC39A/ZIPs) which *import* zinc ions into the cytosolic compartment from the extracellular

space or intracellular vesicles; (ii) Solute Carrier 30 family/ Zinc transporters (SLC30/ZnTs) which *export* zinc ions from the cytosolic compartment to the extracellular space, or intracellular vesicles; and (iii) metallothioneins (MTs) which have a high zinc binding capacity, thus playing key roles in intracellular zinc storage and buffering. To-date, 14 ZIPs, 10 ZnTs, and 4 isoforms of MTs with multiple subtypes/variants have been described in mammals (Kambe et al. 2021).

ZIPs have been identified as playing major roles in a broad array of vital functions and diseases (Takagishi et al. 2017). Their expression and functional roles in vascular physiology and diseases have been paid diminutive attention (Zalewski et al. 2019) until the recent ground-breaking finding that ZIP12 is at least partly responsible for hypoxia-induced PAH in both human and rats (Zhao et al. 2015), inspiring other studies into this field (Tran et al. 2021; Xiao et al. 2021; Zhu et al. 2022). Data on vascular expression and functions of other members of the zinc regulation system remains scant. ZIP14 was shown to mediate influx of Zn^{2+} in sheep pulmonary artery endothelial cells, which may act together with MT to protect from LPS-induced apoptosis (Thambiayya et al., 2012). MT expression and anti-oxidative stress functions in vasculature have been implicated in a number of studies using models of cultured endothelial cells (Kaji et al. 1993; Conway et al. 2010; Thambiayya et al. 2012; Fujie et al. 2020). Thus, despite a growing interest into the zinc regulation system in vascular health and diseases, the understanding of vascular expression and functions of ZIPs, ZnTs and MTs *in vivo* remain a large gap in our knowledge. A systematic, background analysis of the zinc regulation system in human vasculature would benefit further investigations in this field.

Following on from our previous study (Abdo et al. 2021) aiming to characterize the zinc regulation system in human vasculature, in this study we employed multifluorescence quantitative confocal microscopy (MQCM) to investigate immunoreactivities of human microvessels in paraffin tissue sections for multiple ZIPs and MTs. Their detailed distribution among the major cell types of microvessels and association with microvascular morphology and expression of vascular function-related molecules were investigated.

Materials And Methods

Antibodies

A homemade ZIP1 polyclonal antibody (pAb) raised in sheep against the N-terminal sequence was used at 1:100 (immunoblots and antigen/antibody competition data to confirm the antibody specificity were published in Michalczyk and Ackland, 2013). All the remaining antibodies were commercial. A Santa Cruz goat pAb to ZIP1 (affinity purified, immunogen was a cytoplasmic sequence of mouse ZIP1) was used at 1:50. Rabbit pAbs included Abcam ZIP2 (1:50, affinity purified with immunogen which was an intracellular sequence, immunoblot shown by the manufacturer); Novus ZIP2 (1:20, intracellular sequence, immunogen affinity purified); Sigma-Aldrich ZIP8 (1:50, immunogen undisclosed, affinity isolated), Abcam ZIP9 (1:30, internal sequence, immunogen affinity purified); Abcam ZIP10 (1:100, internal sequence, immunogen affinity purified); Abcam ZIP12 (1:50, N-terminal sequence, immunogen

affinity purified, immunoblots published previously in Tran et al. 2021), Abcam ZIP14 (1:50, synthetic 15 amino acid peptide from the internal region; immunogen affinity purified, immunoblot not tested); and Sigma-Aldrich MT3 (1:50, immunogen undisclosed, affinity purified). Monoclonal antibodies (mAbs) used in this study included Abcam ZIP6 (1:25, rabbit recombinant mAb, immunogen undisclosed); Abcam MT1 (1:100, mouse mAb, immunogen was a full length protein, immunoblot shown by the manufacturer), and Dako MT1/2 (1:40, mouse mAb, immunogen undisclosed).

Endothelin-1 (ET-1) goat pAb was from Santa Cruz (1:50, internal sequence, immunoblot shown by the manufacturer). Endothelial nitric oxide synthase (eNOS) mouse mAb from BD (1:50, aa. 1025–1203 sequence, immunoblot shown by the manufacturer). p38 MAPK and its active form p38 MAPK-P (phosphorylated at Threonin 180/Tyrosine 182) rabbit pAbs were obtained from Cell Signalling (both at 1:50, immunoblots published previously in Harper et al 2016). Hypoxia-inducible factor-1α (HIF-1α) mouse mAb clone 54/HIF-1a from BD (1:20, knockout validated). Bone morphogenic protein receptor type 2 (BMPR2) goat polyclonal antibody was from Santa Cruz (1:50, immunoblots published previously in Harper et al. 2019).

Secondary antibodies (all donkey IgG F(ab')2 fragments, absorbed against cross-species reactivities) were from Jackson ImmunoResearch, including anti-rabbit IgG-AF594; anti-goat IgG-AF488; anti-mouse IgG-AF647, used at 1:200. For alternative combinations of primary antibodies in some experiments conjugates were switched colours (anti-rabbit IgG-AF488, anti-goat IgG-AF594, anti-goat IgG-AF647, and anti-mouse IgG-AF488).

Human tissue samples

Subcutaneous tissue biopsies were collected from 14 patients undergoing hernia reconstructive surgeries at The Queen Elizabeth Hospital in Adelaide, Australia. Informed consent was obtained from each donor, utilising protocols approved by the Central Adelaide Local Health Network Human Research Ethics Committee at The Queen Elizabeth Hospital (approval number 2009012). By the ethic approval, individual patient demographic data and their disease status were known only to three authors, RJ, JB and PZ.

Tissue processing and histology

Tissue samples were kept in RPMI medium on ice for less than 2 hours, before the tissue was fixed with 10% formalin in phosphate saline-buffered for 24 hours before processing into paraffin blocks. For quantitative analysis, sections from multiple paraffin blocks were cut to 5 μm thickness and mounted onto tissue arrays for batch analysis of all samples.

Tissue sections were stained with H&E in a standard protocol at the Histopathology service at Adelaide Health and Medical Sciences, then scanned at a 40x objective with a Nanozoomer digital slide scanner (Hamamatsu Photonics, Hamamatsu, Shizuoka, Japan).

Multifluorescence quantitative confocal microscopy (MQCM)

Immunofluorescence of human paraffin tissue sections was performed following a protocol described in our previous study (Tran et al. 2021). MQCM was carried out using an Olympus confocal microscopy system (Olympus FV3000, Tokyo, Japan) and the ImageJ morphometric software (NIH, MA, USA) as previously described (Tran et al. 2021). Briefly, 10 optical fields containing microvessels were serially captured from each biopsy under a 60x silicone-immersed objective, simultaneously in four fluorescence channels set for AF488, AF594, AF647 and DAPI. All microvessels of diameters 20–100 μm in each frame were then selected, their areas in monochromatic images measured for mean fluorescence intensities (MFI) by ImageJ. The fluorescence intensities were quantified with correction for background fluorescence measured by ImageJ in the same experiment for each channel. For punctate immunofluorescence of ET-1, particle counting function was carried out in a predetermined threshold band (70, while maximum intensities varying between 44–154 in the AF488 channel) to uniformly gate in only bright particles sizing of > 10 square pixels (> 3.13 μm^2). Numbers of particles counted in a vascular area were then normalized by numbers of nuclei counted in the DAPI channel in the same area. Microvessels were subdivided into two subpopulations, 'muscularized' when having walls consisting of at least two cell layers in the whole perimeter, and 'non-muscularized' for walls consisting of less than two layers. The percentage of 'muscularized' microvessels varied between zero and ~ 60%.

Statistical analysis

Statistical analysis was undertaken using the Prism 9 software (GraphPad Software, CA, USA). For difference between subgroups of microvessels, a paired two-tailed Wilcoxon test was used. Changes were considered statistically significant at $p < 0.05$.

Results

Patient Characteristics

Tissues donated from 14 patients (10 males, age range: 23–91 years) undergoing hernia reconstructive surgeries were analysed. Their demographic characteristics, body/mass index, usage of vitamin or zinc supplements, cigarette smoking status, and history of pathologic conditions known at the time of surgeries are summarized in Supporting Information Table S1. Cardiovascular diseases were reported in 4 cases (infarct, 1; deep thrombosis of lower extremity, 1). Conditions that may be risk factors to cardiovascular diseases included hypertension (2), diabetes (3), asthmas (2) and COPD (1). Nil history was reported for 4.

Morphology of human subcutaneous microvessels

In H&E staining subcutaneous biopsies consisted of mostly adipocytes, scattered with islands of dense irregular connective tissue, nerve fibres and microvessels. By applying the inclusion criteria of diameters between 20 to 100 μm, the selected microvessels included both venules and arterioles but excluded much smaller capillaries (< 10 μm by definition). The microvessels varied in their wall thickness and relative degree of muscularization (Fig. 1). Muscularized microvessels showed increased wall-to-lumen

projection, often having rough endothelial surfaces, increased nuclear density and fibrotic staining in the tunica intima (Fig. 1a, b).

At high resolution confocal microscopy, microvascular cell layers of tunica intima (endothelium) and tunica media (smooth muscle) could clearly be demarcated, allowing for sub-classification by degree of muscularization (Fig. 1c).

Localization of multiple ZIPs and MTs in human microvasculature

Preliminary experiments were carried out to titrate primary antibodies and define optimal dilutions, as described in the Methods. In the conditions of our protocols, similar patterns of ZIP1 immunofluorescence in the endothelium and smooth muscle were detected by a homemade sheep antibody (Michalczyk and Ackland 2013) and a commercial goat antibody (Fig. 2a). For ZIP2, similar patterns of endothelium and smooth muscle staining were detected using the two rabbit polyclonal antibodies (Abcam and Novus, Fig. 2a). Other ZIPs detected in microvessels were ZIP8, ZIP10, ZIP12 and ZIP14 (Figs. 1b, 2b). The Abcam antibodies to ZIP6 and ZIP9 did not stain the vasculature in the described protocol even at the highest tested concentration.

Next, all the three tested antibodies to MTs revealed moderate to bright immunoreactivities in human microvessels (Fig. 3).

High resolution by confocal microscopy allowed detail localization of ZIPs and MTs, roughly equally in both endothelium and smooth muscle (ZIP10, ZIP14, MT1, MT1/2), or relatively more abundantly in endothelium (ZIP1, ZIP2, ZIP8, ZIP12), or smooth muscle (MT3) (Figs. 1b, 2, 3). Immunofluorescence of ZIPs showed both cytoplasmic and membrane-like patterns, the latter was particularly distinctive for ZIP1 and ZIP12. While all tested MTs revealed cytoplasmic patterns, the mAb to MT1 also detected bright nucleolar staining while the MT1/2 mAb detected a lesser level of nucleolar staining (Fig. 3).

Changes of ZIP and MT immunoreactivities associated with microvascular muscularization

The limited number of patients and heterogeneity of their history would not allow for a quantitative analysis of potential changes of ZIP/MT immunoreactivities by disease, or by age/gender subgroups. However, a distinctive variation of ZIP1, ZIP2, ZIP12 and MT3 among microvessels of the same donor led us to a hypothesis that there are changes associated with microvascular morphology. For the purpose of quantitative analysis, the relatively “muscularized” were discerned from “non-muscularized” microvessels, arbitrarily based on whether their wall contained at least two muscle cell layers throughout their perimeters. The microvascular immunoreactivities of ZIP1, ZIP2, ZIP12 and MT3 quantified by their mean fluorescence intensities confirmed statistically significant increases in muscularized vs. non-muscularized microvessels (Figs. 4, 5). Of note, while upregulated ZIP1, ZIP2 and ZIP12 were recorded mostly in the endothelium, increased MT3 was mostly seen in the smooth muscle compartment.

Change in microvascular muscularization was associated with vascular function-related molecules

Next, we tested if muscularized and non-muscularized subpopulations of microvessels would display any difference in regard to expression and localization of molecules that have previously recognized roles in vascular functions. A panel of function-related markers was investigated including eNOS, ET-1, HIF-1α, α-SMA, and p38 MAPK. As expected, while the α-SMA immunoreactivity was localized specifically to the smooth muscle (Fig. 5a), most of ET-1 (Fig. 4b) and eNOS (Fig. 6a) were localized to the endothelium. Notably, punctate ET-1 immunofluorescence could be visualized in endothelial-smooth muscle junctions, on the endothelial side (Fig. 4b). HIF-1α was mostly localized to the endothelium (Fig. 6a). Interestingly, while staining with an antibody to the total p38 MAPK detected bright immunoreactivity in both smooth muscle and endothelium, the active form p38 MAPK-P was mostly localized to the latter (Supporting Information Figure S1).

Importantly, ET-1, MT3 and p38 MAPK-P in quantitative analysis revealed significant increases in muscularized microvessels. Although eNOS and HIF-α also showed a strong variation among microvessels of the same donor, their overall change among all donors was not statistically significant, increasing with muscularization in some donors but decreasing in others (Fig. 6b).

Discussion

To our best knowledge this work is the first *in vivo* description of protein expression of multiple ZIPs and MTs in human microvasculature. A complete list analysis of the ZIPs and MTs, and the third family of zinc regulation proteins, SLC30As/ZnTs remains however a task for future investigations. Despite a limitation that expression at the gene level was not analysed, protein expression of multiple members of ZIPs and MTs supports a hypothesis that there is a redundancy in zinc regulation system which may be required for a tight control of zinc homeostasis in vascular functions. As another limitation, immunofluorescence results should be interpreted with caution on antibodies' specificity; to minimize this, most of the primary antibodies used in this study were tested independently by Western blots or immunogen/antibody competition in our previous publications, or published by the manufacturers.

Results of this study are mostly in line with our previous data on gene expression in primary cell culture (Abdo et al. 2021), with exceptions as discussed below. Thus, while abundant mRNA expression was found in primary cell cultures for ZIP6 and ZIP9, their protein expression in this study could not be detected in microvessels from subcutaneous biopsies. Furthermore, while the relative abundance of gene expression in cell cultures was low for ZIP2, ZIP12 and MT3, protein immunoreactivities in microvascular tissues were varying, brighter in subpopulation(s) of microvessels. Apart from a potential sensitivity issue that could not be ruled out, one possible cause was that while mRNA data was obtained from primary cells of aorta and pulmonary artery, protein expression data was from *in vivo* sampling of microvessels. Furthermore, while primary cell culture data reflected a normal state in which vascular cells expressed minimal levels of ZIP2, ZIP12 and MT3, biopsies included pathological conditions that could induce

these proteins. In accordance with this, previous data provides multiple evidence that ZIP12 could be induced *in vivo* in vasculature in human patients and rat models of PAH (Zhao et al. 2015; Tran et al. 2021; Xiao et al. 2021). *In vitro*, both ZIP2 and ZIP12 were shown induced at mRNA and protein levels in vascular cells by depletion of zinc (Abdo et al. 2021). The tissue localization data in this study was in line with previous studies (Zhao et al. 2015; Abdo et al. 2021; Tran et al. 2021); ZIP12 was localized to both the endothelial and smooth muscle cell types of the vascular wall. Microvascular expression of ZIP14 was consistent with previous data, that influx of labile zinc in cultured sheep pulmonary artery endothelial cells was sensitive to ZIP14 siRNA indicating the presence of functional ZIP14 in this cell type (Thambiayya et al. 2012). Our findings of highly expressed ZIP1 in microvessels was in line with a notion that ZIP1 is expressed ubiquitously across cell types (Schweigel-Röntgen 2014). Regarding other ZIPs, to our knowledge ours is the first study to examine their localization in vascular walls.

Known as free radical scavengers, MTs are surrogate markers of oxidative stress and indicators of labile intracellular zinc levels (Mareiro et al. 2017). MTs have been studied in various cell culture models of vascular endothelial cells in oxidative stress associated with exposure to heavy metals, or other stress stimuli (Kaji et al. 1993; Conway et al. 2010; Thambiayya et al. 2012; Fujie et al. 2020; Rubiolo et al. 2021). Metallothioneins have also been commonly reported to be elevated in PAH patients as well as in experimental models of PAH (Maarman 2018). *In vitro* studies showed that MT can respond to nitride oxide (free radical and vasodilator mediator) by releasing Zn2 + ions (Kroncke et al. 1994; Thambiayya et al. 2012), which could be relevant to a mechanism of vasodilation. Surprisingly MT expression and functions in the other vascular cell type namely smooth muscle have been paid little attention. In a rare report, using immunohistochemical staining and immunogold electron microscopy, it was noted that most of the MT induced in human atherosclerotic lesions was localized to the vascular smooth muscle cells (Göbel et al. 2000). Our finding of smooth muscle as the major harbour of MTs in the microvascular wall further puts this cell type in the spotlight of future investigations into vascular zinc biology.

As a rationale for differential analysis of quantitative data in muscularized vs. non-muscularized microvessels, increased proliferation (i.e. exit from the normally quiescent state) of smooth muscle is considered a key process in vascular pathology, e.g. in atherosclerosis (Sedding et al. 2018) and diabetic vascular restenosis (Moshapa et al. 2019). In studies of PAH, increased levels of lung microvascular muscularization serve as an indicator of pathologic changes leading to resistance and increased pulmonary blood pressure (Zhao et al. 2015; Harper et al. 2019; Maietta et al. 2021). In this study, the large heterogeneity of expression of zinc regulation proteins in subcutaneous microvessels was found to be associated with their state of muscularization, in particular for ZIP1, ZIP2, ZIP12 and MT3. The difference in muscularization could at least partially be contributed by arteriole-vs-venule difference, which could not be accessed without exact localization of microvessels prior or posterior to capillary circulation. Therefore, we could not precisely ascribe the upregulated expression of the above-mentioned proteins to arterioles vs. venules.

The differences between the two microvessels subpopulations in their expression of vascular-active molecules, however, give a notable indication on functional differentiation, in addition to morphologic

features. Known primarily as a potent vasoconstrictor, ET-1 has broad effects on various pathways critical for vascular functions and diseases e.g. induction of VCAM-1 (Ishizuka 1999), pro-inflammatory activation of leucocytes including neutrophils (Kaszaki et al., 2008) and macrophages (Zhang et al. 2021). Relevant to the vascular pathology, ET-1 was reported to activate smooth muscle by stimulating protein synthesis, promoting proliferation and hypertrophy of pulmonary arterial smooth muscle cells (Chua et al. 1992; Zamora et al. 1993). In this study increased particulate immunofluorescence of ET-1 in muscularized microvessels was localized to endothelial-smooth muscle junctions, supporting a hypothesis that paracrine ET-1-mediated endothelial-smooth muscle crosstalk may be required for not only vasoconstriction, but also proliferation of vascular smooth muscle. As a marker of both endothelial-mesenchymal transition and vascular remodelling, increased α-SMA expression is known to be associated with exposure to mechanical stress that could also induce activation of p38 MAPK (Wang et al. 2006). In a study of mechanisms leading to PAH, activation of p38 MAPK was found to be associated with oxidative stress and inflammation (Church et al. 2015). Thus, data presented here argues that upregulation of zinc regulation proteins ZIP1, ZIP2, ZIP2 and MT3 is associated with a functionally activated state, compared to a relatively quiescent state of microvessels.

Conclusion

In conclusion, this study provides background data of protein expression and localization of multiple ZIPs and MTs in endothelial and smooth muscle layers of human microvascular walls. The presented data supports a hypothesis that the zinc regulation system in the human microvasculature, in particular the ZIP1, ZIP2, ZIP12 and MT3 proteins, plays an important role in microvascular physiology and could be a therapeutic target for diseases that involve microvascular remodelling.

Declarations

Acknowledgement We thank Ms Agatha Labrinidis and the staff of Adelaide Microscopy at the University of Adelaide, Dr James Manavis and the staff of the Histopathology Service at the Adelaide Health and Medical Sciences, Mr Hong Liu and Mr Matthew G Macowan from the Royal Adelaide Hospital Department of Thoracic Medicine for their excellent technical assistance.

Funding HBT, RJ, AA, JB, SH and PZ were supported by NHMRC APP1138917 (CIA PZ). PR was supported by NHMRC APP1147619 (CIA PR). The funding sources had no role in study design, data collection, analysis or interpretation of the data, writing the final report, or the decision to submit the article for publication.

Conflict of interest The authors declare that they have no competing interests.

Data availability All the data supporting the findings of this study are available within the article and its supplementary materials.

Author contribution HBT: conception and design of the study, acquisition, analysis and interpretation of data, draft and final approval of the manuscript; RJ: sample acquisition, critical review of the manuscript and final approval of the version to be published; AA and PA: analysis of data, critical review of the manuscript and final approval of the version to be published; PR: interpretation of data, critical review of the manuscript and final approval of the version to be published; JB: sample acquisition, interpretation of data, critical review of the manuscript and final approval of the version to be published; SH: interpretation of data, critical review of the manuscript and final approval of the version to be published; PZ: conception of the study, interpretation of data, critical review of the manuscript and final approval of the version to be published.

References

1. Abdo AI, Tran HB, Hodge S, Beltrame JF, Zalewski P. (2020). Zinc homeostasis alters zinc transporter protein expression in vascular endothelial and smooth muscle cells. Biol Trace Elem Res 199, 2158–2171. https://doi:10.1007/s12011-020-02328-z.
2. Bkaily G, Abdallah AN, Simon Y, Jazzar A, Jacques D. (2021). Vascular smooth muscle remodelling in health and disease. Can J Physiol and Pharmacol 11:171–178. https://doi:10.1139/cjpp-2020-0399
3. Chua BH, Krebs CJ, Chua CC, Diglio CA. (1992). Endothelin stimulates protein synthesis in smooth muscle cells. Am J Physiol Endocrinol Metab 262(4):E412–E416. https://doi:10.1152/ajpendo.1992.262.4.E412.
4. Church AC, Martin DH, Wadsworth R, Bryson G, Fisher AJ, … Peacock AJ (2015). The reversal of pulmonary vascular remodeling through inhibition of p38 MAPK-a: a potential novel anti-inflammatory strategy in pulmonary hypertension. A J Physiol Lung Cell Mol Physiol 309:L333–L347. https://doi:10.1152/ajplung.00038.2015.
5. Conway DE, Lee S, Eskin SG, Shah AK, Jo H, McIntire LV. (2010). Endothelial metallothionein expression and intracellular free zinc levels are regulated by shear stress (2010). Am J Physiol Cell Physiol 299(6):C1461-7. https://doi:10.1152/ajpcell.00570.2009.
6. Fujie T, Ozaki Y, Takenaka F, Nishio M, Hara T, Fujiwara Y, Kaji T. (2020). Induction of metallothionein isoforms in cultured bovine aortic endothelial cells exposed to cadmium. J Toxicol Sci 45(12):801–806. https://doi:10.2131/jts.45.801.
7. Göbel H, van der Wal AC, Teeling P, van der Loos CM, Becker AE. (2000). Metallothionein in human atherosclerotic lesions: a scavenger mechanism for reactive oxygen species in the plaque? Virchows Arch, 437(5):528–33. https://doi:10.1007/s004280000260.
8. Harper RL, Maiolo S, Ward RJ, Seyfang J, Cockshell MP, Bonder CS, Reynolds PN. (2019). BMPR2-expressing bone marrow-derived endothelial-like progenitor cells alleviate pulmonary arterial hypertension in vivo. Respirology 24(11):1095–1103. https://doi:10.1111/resp.13552.
9. Harper RL, Reynolds AM, Bonder CS, Reynolds PN (2016). BMPR2 gene therapy for PAH acts via Smad and non-Smad signalling. Respirology 21(4):727–33. https://doi:10.1111/resp.12729.

10. Ishizuka T, Takamizawa-Matsumoto M, Suzuki K, Kurita A. (1999). Endothelin-1 enhances vascular cell adhesion molecule-1 expression in tumor necrosis factor alpha-stimulated vascular endothelial cells. *Eur J Pharmacol* 369 (1999) 237–245. https://doi:10.1016/s0014-2999(99)00042-4.
11. Kaji T, Yamamoto C, Tsubaki S, Ohkawara S, Sakamoto M, Sato M, Kozuka H (1993). Metallothionein induction by cadmium, cytokines, thrombin and endothelin-1 in cultured vascular endothelial cells. Life Sci 53(15):1185–91. https://doi:10.1016/0024-3205(93)90536-c.
12. Kambe T, Taylor KM, Fu D. Zinc transporters and their functional integration in mammalian cells. J Biol Chem 296:100320. https://doi:10.1016/j.jbc.2021.100320.
13. Kaszaki J, Czóbel M, Szalay L, Nagy S, Boros M (2008). Endothelin-1 induces organ-specific histamine liberation and neutrophil granulocyte accumulation in the rat. Inflamm Res, 57(8):396–402. https://doi:10.1007/s00011-007-7224-x.
14. Kröncke KD, Fehsel K, Schmidt T, Zenke FT, Dasting I, Wesener JR, … Kolb-Bachofen V (1994). Nitric oxide destroys zinc-sulfur clusters inducing zinc release from metallothionein and inhibition of the zinc finger-type yeast transcription activator LAC9. Biochem Biophys Res Commun 200(2):1105–10. https://doi:10.1006/bbrc.1994.1564.
15. Lambazi H, Trask AJ (2017). Coronary microvascular disease as an early culprit in the pathophysiology of diabetes and metabolic syndrome. Pharmacol Res 123: 114–121. https://doi:10.1016/j.phrs.2017.07.004.
16. Liu P, Gu Y, Luo J, Ye P, Zheng Y, Yu W, Chen S (2019). Inhibition of Src activation reverses pulmonary vascular remodeling in experimental pulmonary arterial hypertension via Akt/mTOR/HIF-1 signaling pathway. Exp Cell Res 380(1):36–46. https://doi:10.1016/j.yexcr.2019.02.022.
17. Maarman GJ (2018). Pulmonary arterial hypertension and the potential roles of metallothioneins: A focused review. Life Sci 214:77–83. https://europepmc.org/article/med/30355531
18. Maietta V, Reyes-García J, Yadav VR, Zheng Y-M, Peng X, Wang YX. (2021). Cellular and molecular processes in pulmonary hypertension. Adv Exp Med Biol 1304:21–38. https://doi:10.1007/978-3-030-68748-9_2.
19. Marreiro DD, Cruz KJ, Morais JB, Beserra JB, Severo JS, de Oliveira AR (2017). Zinc and oxidative stress: Current mechanisms. Antioxidants 6(2);pii:E24. https://doi:10.3390/antiox6020024.
20. Michalczyk AA, Ackland ML (2013). hZIP1 (hSLC39A1) regulates zinc homeostasis in gut epithelial cells. Genes Nutr 8(5):475–86. https://doi:10.1007/s12263-013-0332-z.
21. Moshapa FT, Riches-Suman K, Palmer TM (2019). Therapeutic targeting of the proinflammatory IL-6-JAK/STAT signalling pathways responsible for vascular restenosis in type 2 diabetes mellitus. Cardiol Res Pract 2019:9846312. https://doi:10.1155/2019/9846312.
22. Mulvany MJ (1999). Vascular remodelling of resistance vessels: can we define this? Cardiovasc Res 41(1):9–13. https://doi.org/10.1016/S0008-6363(98)00289-2.
23. Ouarné M, Pena A, Franco CA (2021). From remodeling to quiescence: The transformation of the vascular network. Cells Dev 203735. https://doi:10.1016/j.cdev.2021.203735.

24. Ranasinghe ADCU, Lee DD, Schwarz MA (2020). Mechanistic regulation of SPHK1 expression and translocation by EMAP II in pulmonary smooth muscle cells. Biochim Biophys Acta Mol Cell Biol Lipids 1865(12):158789. https://doi:10.1016/j.bbalip.2020.158789.
25. Ricard N, Bailly S., Guignabert, C., & Simons, M. (2021). The quiescent endothelium: signalling pathways regulating organ-specific endothelial normalcy. Nat Rev Cardiol. 18(8):565–580. https://doi:10.1038/s41569-021-00517-4.
26. Rubiolo JA, Lence E, González-Bello C, Roel M, Gil-Longo J, Campos-Toimil M,… Botana LM (2021). Crambescin C1 acts as a possible substrate of iNOS and eNOS increasing nitric oxide production and inducing in vivo hypotensive effect. Front Pharmacol 12:694639. https://doi:10.3389/fphar.2021.694639.
27. Schweigel-Röntgen M (2014). The families of zinc (SLC30 and SLC39) and copper (SLC31) transporters. Curr Top Membr 73:321 – 55. https://doi:10.1016/B978-0-12-800223-0.00009-8.
28. Sedding DG, Boyle EC, Demandt JAF, Sluimer JC, Dutzmann J, Haverich A, Bauersachs J (2018). Vasa vasorum angiogenesis: key player in the initiation and progression of atherosclerosis and potential target for the treatment of cardiovascular disease. Front Immunol, 9:706. https://doi:10.3389/fimmu.2018.00706.
29. Takagishi T, Hara T, Fukada T (2017). Recent Advances in the Role of SLC39A/ZIP Zinc Transporters In Vivo. Int J Mol Sci 18(12):2708. https://doi:10.3390/ijms18122708
30. Thambiayya K, Wasserloos K, Kagan VE, Stoyanovsky D, Pitt BR (2012). A critical role for increased labiled zinc in reducing sensitivity of cultured sheep pulmonary artery endothelial cells to LPS-induced apoptosis. Am J Physiol Lung Cell Mol Physiol, 302(12):L1287-95. https://doi:10.1152/ajplung.00385.2011.
31. Tran HB, Maiolo S, Harper R, Zalewski PD, Reynolds P, Hodge S (2021). Dysregulated zinc and sphingosine-1-phosphate signalling in pulmonary hypertension: potential effects by targeting of bone morphogenetic protein receptor type 2 in pulmonary microvessels. Cell Biol Int 45(11):2368–2379. https://doi:10.1002/cbin.11682.
32. Wang J, Zohar R, McCulloch CA (2006). Multiple roles of alpha-smooth muscle actin in mechanotransduction. Exp Cell Res 312(3):205–14. https://doi:10.1016/j.yexcr.2005.11.004.
33. Xiao G, Lian G, Wang T, Chen W, Zhuang W, Luo L,… Xie L. (2021). Zinc-mediated activation of CREB pathway in proliferation of pulmonary artery smooth muscle cells in pulmonary hypertension. Cell Commun Signal 19(1):103. https://doi:10.1186/s12964-021-00779-y.
34. Zalewski PD, Beltrame JF, Wawer AA, Abdo AI, Murgia C (2019). Roles for endothelial zinc homeostasis in vascular physiology and coronary artery disease. Crit Rev Food Sci Nutr 59(21):3511–3525. https://doi:10.1080/10408398.2018.1495614.
35. Zamora MA, Dempsey EC, Walchak SJ, Stelzner TJ (1993). BQ123, an ETA receptor antagonist, inhibits endothelin-1-mediated proliferation of human pulmonary artery smooth muscle cells. Am J Respir Cell Mol Physiol 9(4):429–433. https://doi:10.1165/ajrcmb/9.4.429.

36. Zhang J, Zhao WS, Xu L, Wang X, Li XL, Yang XC (2021). Endothelium-specific endothelin-1 expression promotes pro-inflammatory macrophage activation by regulating miR-33/NR4A axis. Exp Cell Res 399(1):112443. https://doi:10.1016/j.yexcr.2020.112443.
37. Zhao L, Oliver E, Maratou K, Atanu SS, Dubois OD, Cotroneo E, … Wilkins MR (2015). The zinc transporter ZIP12 regulates the pulmonary vascular response to chronic hypoxia. Nature, 524(7565):356–60. https://doi:10.1038/nature14620.
38. Zhu T, Wang X, Zheng Z, Quan J, Liu Y, Wang Y,… Zhang Z (2022). ZIP12 contributes to hypoxic pulmonary hypertension by driving phenotypic switching of pulmonary artery smooth muscle cells. J Cardiovasc Pharmacol 79(2):235–243. https://doi:10.1097/FJC.0000000000001156.

Figures

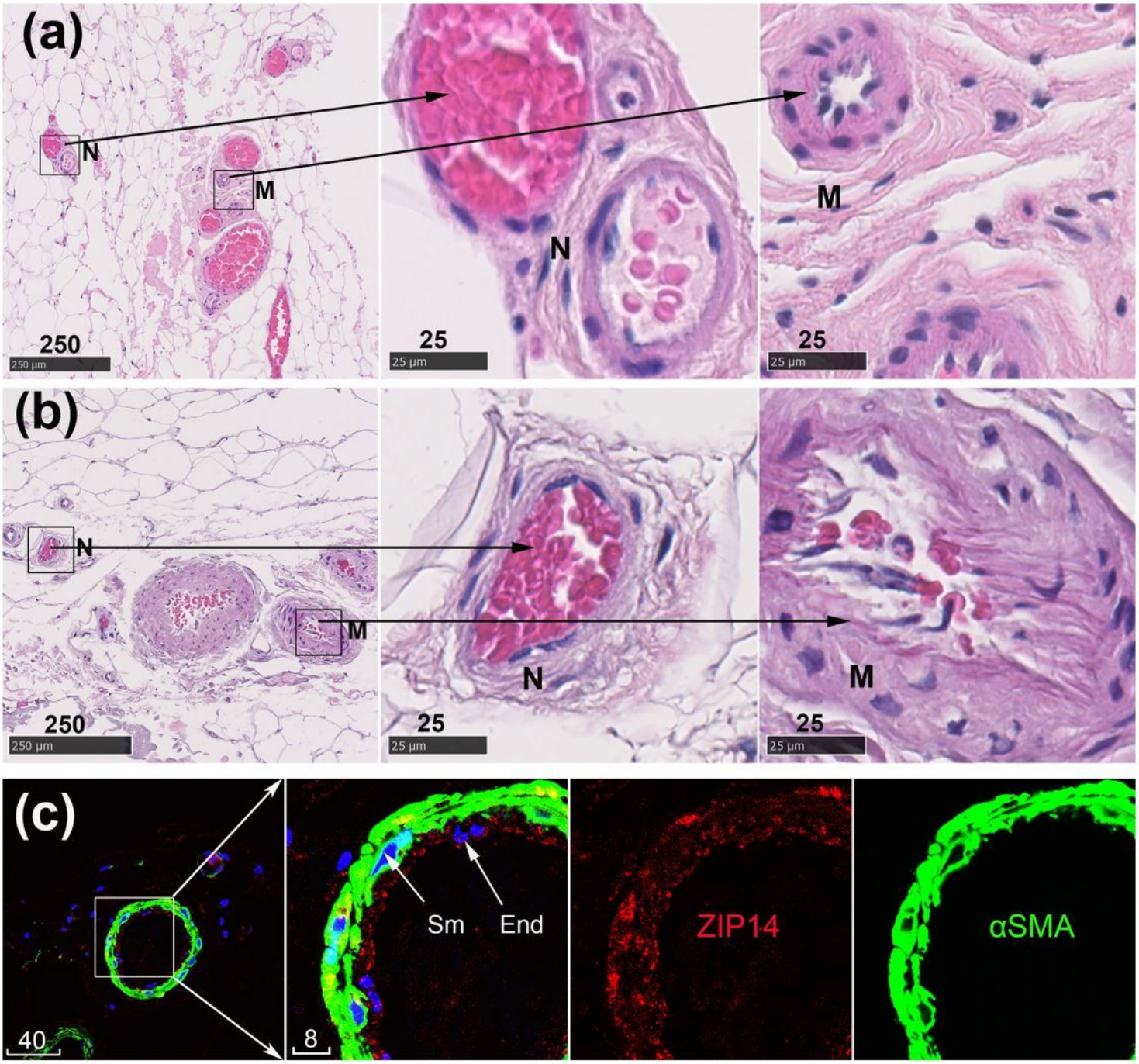

Figure 1

Morphology of human subcutaneous microvessels. (a) and (b) Representative H&E microphotos of microvessels in biopsies of two different donors. Boxed areas are shown to the right at a higher magnification to reveal relatively non-muscularized (N) and muscularized (M) microvessels. (c) A representative multifluorescence confocal image of subcutaneous tissue stained for ZIP14 (red), α-SMA (green) and nuclei (blue, DAPI). The boxed area is shown to the right at a higher magnification, revealing different layers of the microvascular wall: Sm, smooth muscle; End, endothelium. Scale bars are in micrometers

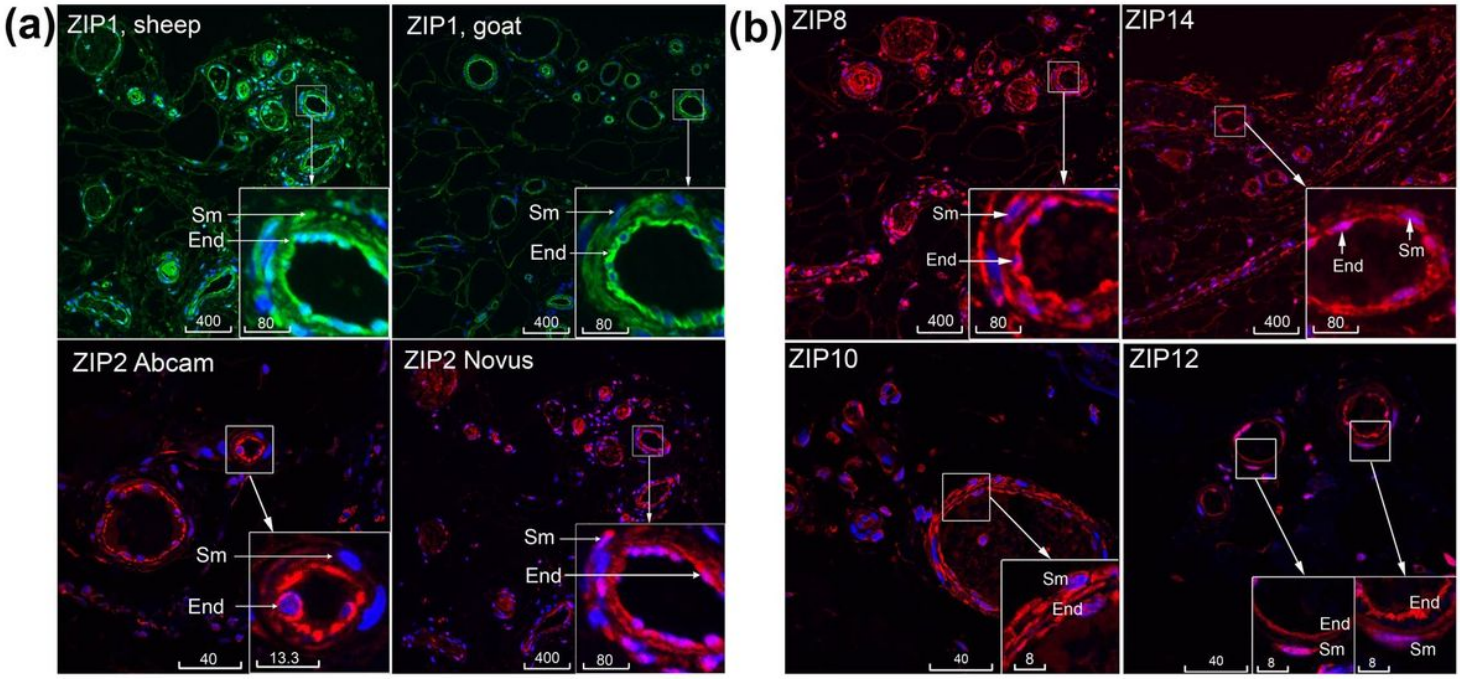

Figure 2

Immunolocalization of multiple ZIPs in microvessels. (a) Comparison of ZIP1 (green) and ZIP2 (red) antibodies from different sources. (b) Immunolocalization of ZIP8, ZIP10, ZIP14 and ZIP12 (all red) in microvessels. Blue is DAPI. Sm, smooth muscle; End, endothelium. Scale bars are in micrometers

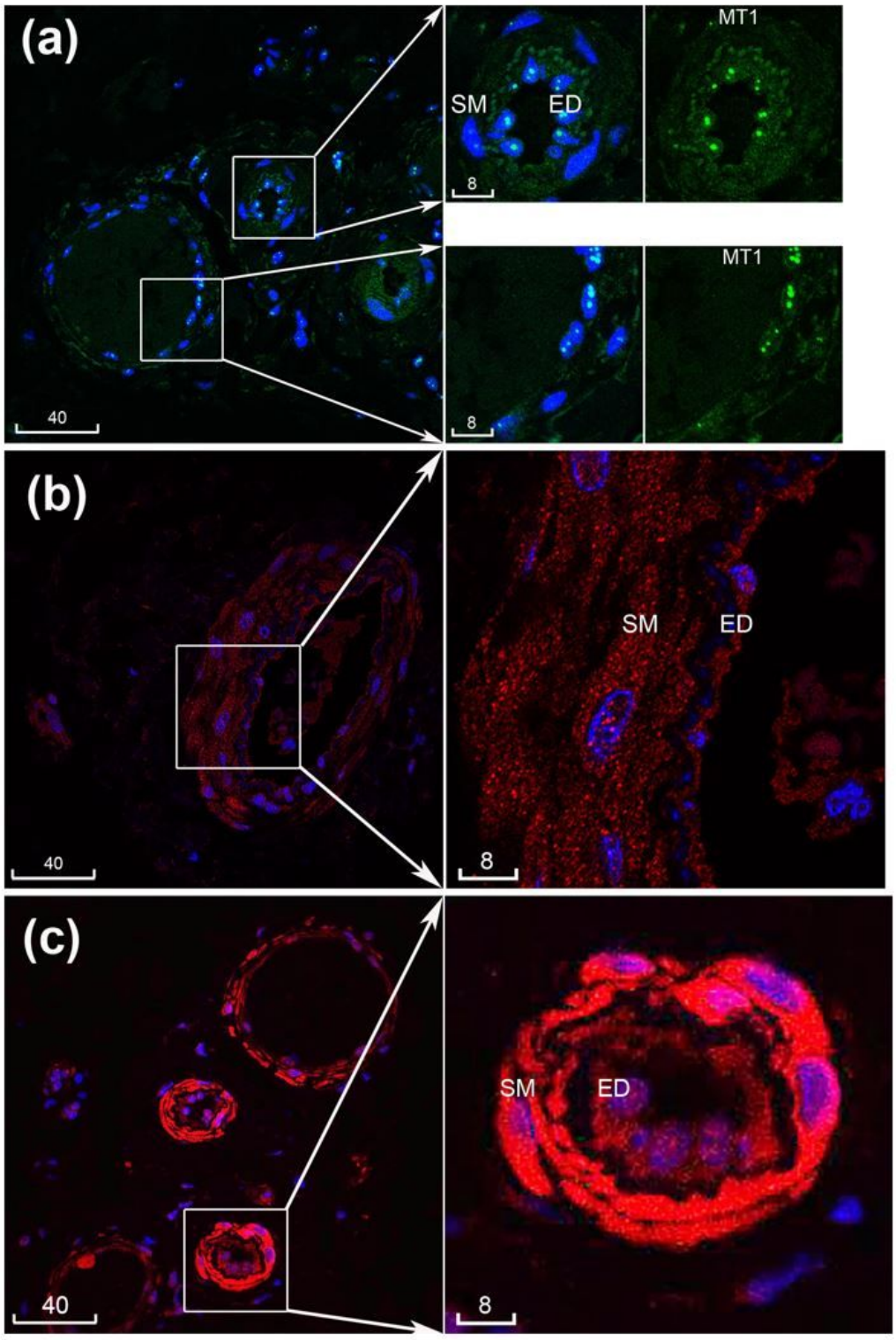

Figure 3

Immunolocalization of multiple metallothioneins in microvessels. (a) MT1 (green); (b) MT1/2 (red); (c) MT3 (red). Blue is DAPI. Sm, smooth muscle; End, endothelium. Scale bars are in micrometers

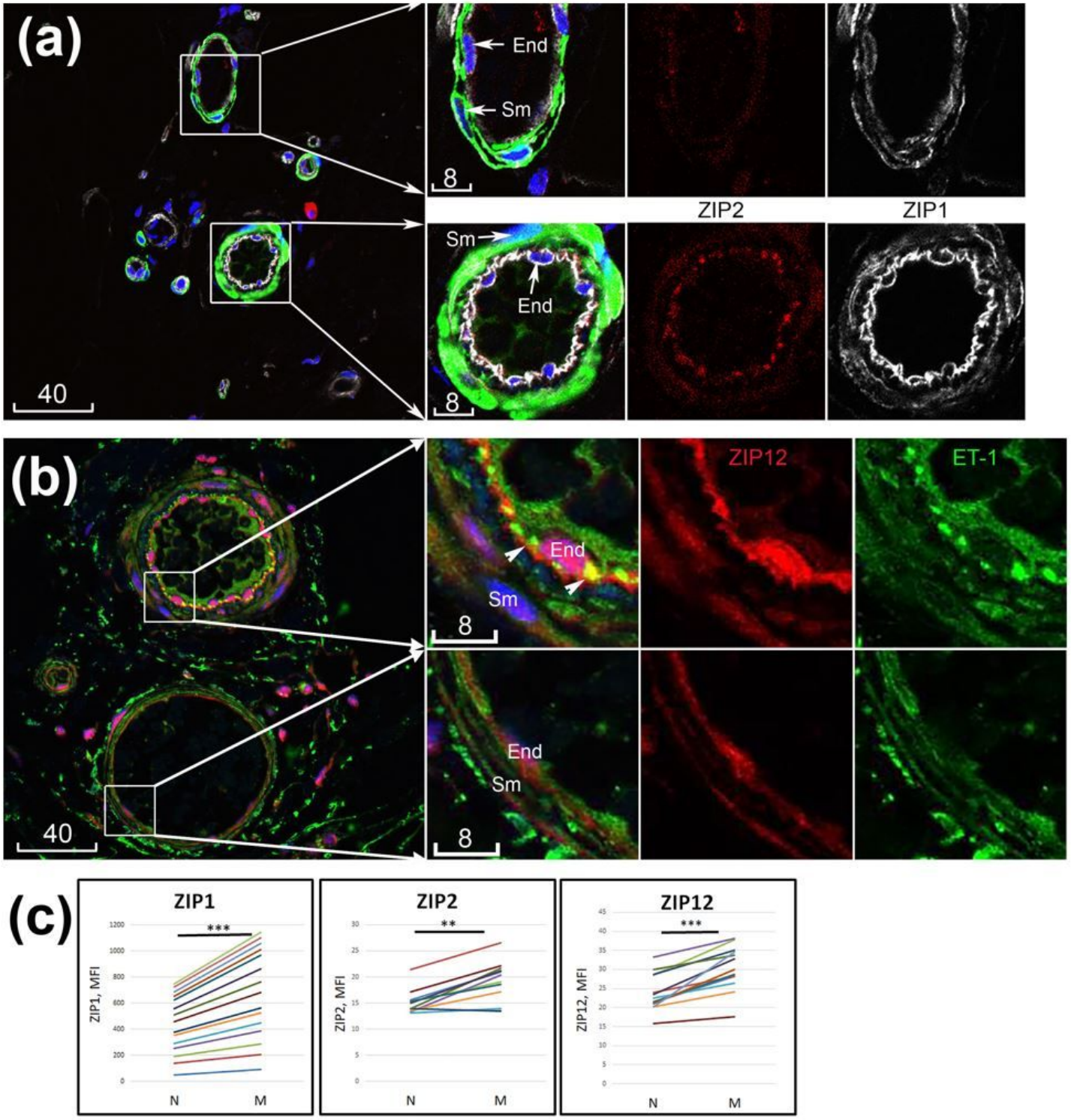

Figure 4

Upregulated immunoreactivities of ZIPs in muscularized vs. non-muscularized microvascular walls. (a) Confocal image of ZIP1 (white) and ZIP2 (red); the two boxed areas shown to the right at higher magnification revealing a relatively non-muscularized (top) vs. muscularized (bottom) microvessels. (b) Confocal image of ZIP12 (red) co-labeled with ET-1 (green, arrowheads point to endothelial-smooth muscle junctions); the two boxed areas shown to the right at higher magnification revealing a relatively

muscularized (top) vs. non-muscularized (bottom) microvessels. Blue is DAPI counterstaining of nuclei. Sm, smooth muscle; End, endothelium. Scale bars are in micrometers. (c) Quantitative measurements of ZIP1, ZIP2 and ZIP12 in non-muscularized (N) vs. muscularized (M) microvessels. **, p=0.01; *** p<0.001

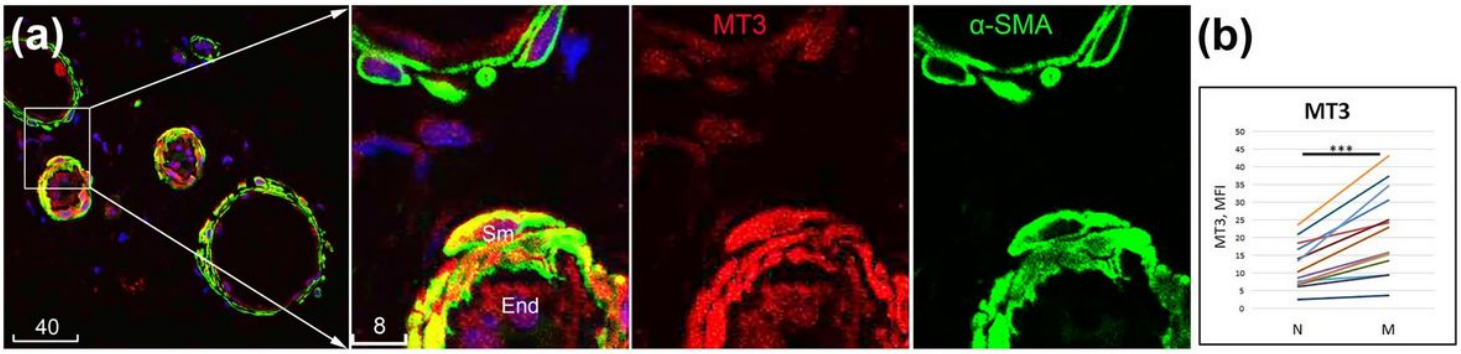

Figure 5

Upregulated immunoreactivity of MT3 in muscularized microvessels. (a) Representative confocal image of MT3 (red) co-labeled with α-SMA (green). The boxed area is shown to the right at a higher magnification to reveal a relatively non-muscularized (top) and muscularized (bottom) microvessels. Blue is DAPI. Sm, smooth muscle; End, endothelium. Scale bars are in micrometers. (b) Quantitative measurements of MT3 immunoreactivities in non-muscularized (N) vs. muscularized (M) microvascular walls. ***, p<0.001

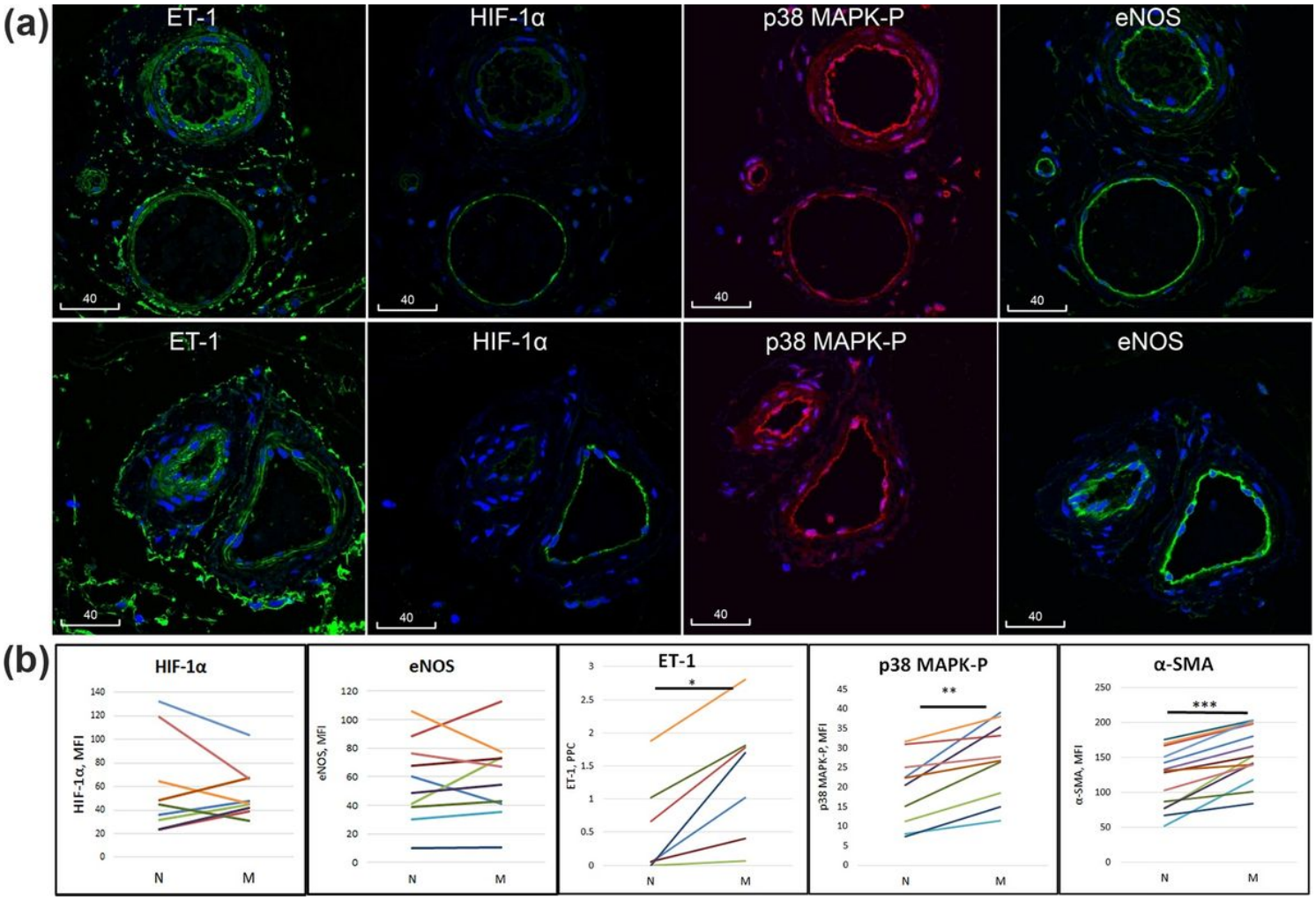

Figure 6

Immunolocalization of function-related proteins and their variation among microvessels of the same donors. (a) Confocal images of adjacent serial sections of microvessels from two representative donors, stained for various function-related molecules. Blue is pseudocolor of DAPI. Scale bars are in micrometers. (b) Quantitation of immunoreactivities in non-muscularized (N) vs muscularized (M) microvessels. *, $p<0.05$; **, $p<0.01$; ***, $p<0.001$

Supplementary Files

This is a list of supplementary files associated with this preprint. Click to download.

- SupportingInformation.pdf